Branching ratio in x-ray absorption spectroscopy

B. T. Thole and G. van der Laan*
Materials Science Center, University of Groningen, Nijenborgh 18, NL-9747 AG Groningen, The Netherlands
(Received 1 February 1988)

The origin of nonstatistical branching ratios in spin-orbit-split x-ray absorption spectra is explained. Atomic calculations for transition metals show a systematic change which is due to initial-state spin-orbit splitting and electrostatic interactions between core hole and valence electrons. We have formulated the results of these atomic calculations in general rules, which are also applicable to solids. In the free atom the branching ratio reaches a maximum for the Hund's-rule ground state and its value decreases gradually for S, L, and J levels of higher energy. The presence of a crystal field results in a lower branching ratio when it produces a low-spin ground state. The rules can be used to assess the spin state and the spin-orbit splitting from the experimental branching ratio in transition-metal and rare-earth compounds. A specific example is given for the influence of second-order spin-orbit interactions in high-spin Ni compounds.

I. INTRODUCTION

Transition-metal, rare-earth, and actinide compounds display large white lines at the threshold for core excitation in x-ray absorption spectroscopy (XAS).[1-3] The recent progress in synchrotron-radiation physics has even permitted resolution of the multiplet structure in some of these white lines. Computational analyses have shown that these multiplets arise from the accessible final states with a core hole and an additional valence electron.[4-8] For example, the $L_{2,3}$ white lines of the first-row transition-metal compounds originate from transitions $3d^n \rightarrow 2p^5 3d^{n+1}$, where the large spin-orbit interaction of the $2p$ core hole splits the final states into two groups with a large energy separation. The total intensity is proportional to the number of valence holes.[9,10] However, the intensity ratio of these two spin-orbit-split lines is not simply given by the statistical value. Experimental studies have shown that the branching ratio $I(L_3)/[I(L_2)+I(L_3)]$ in the $3d$ transition metals changes from 0.41 in Ti to 0.7–0.8 in Mn.[11-14] In the lanthanides the branching ratio $I(M_5)/[I(M_4)+I(M_5)]$ changes from 0.39 in La to 1 in Yb.[8,15,16] Also, at the end of the $4d$ and $5d$ transition metal series the branching ratio deviates from the statistical value.[17-20] Especially interesting is the relation between the branching ratio and the local magnetic moment, which has recently been found in various alloys.[21-23]

These deviations from the statistical branching ratio have in the past been subject for various studies. Mott[24] already suggested that the absence of the L_2 white line in Pt (Ref. 17) was due to the absence of $4d_{3/2}$ character in the valence band. Mattheiss and Dietz[25] have confirmed this idea with a tight-binding calculation. However, the use of such a single-particle model is only justified for other than d^9 configurations if the interactions between the d electrons can be neglected. Fink *et al.*[26] have clearly shown that experimental absorption spectra cannot be explained by the density of unoccupied d states, even when single-particle matrix elements are included.

Onodera[27] showed in a model for the exciton transition $p^6 \rightarrow p^5 s$ in the alkali halides that also electrostatic interactions between core hole and valence electrons can influence the branching ratio. The statistical ratio obtained in the absence of electrostatic interactions in the final state (we will call this the jj coupling limit) gradually changes to the extreme intensity ratio of 0:1, when the core-hole spin-orbit interaction is reduced to zero (LS coupling). This model has been relatively widely applied.[12,28-32] However, this model, which considers only a two-particle final state, always gives an intensity ratio smaller than the statistical value, whereas larger-than-statistical branching ratios have been found experimentally for higher d counts.

Full multiplet calculations in intermediate coupling give generally a good agreement with experimental branching ratios. Examples of this are the calculations in octahedral symmetry for high-spin $3d$ ions by Yamaguchi *et al.*,[5] the multiconfigurational Dirac-Fock calculation by Waddington *et al.*,[33] and the atomic Hartree-Fock calculation for the $4f$ metals by Thole *et al.*[16] However, the complexity of these calculations barred the analysis of the factors which determine the branching ratio.

In order to explain the branching ratio of the white lines, a full atomic approach, including crystal or ligand field, will be necessary, because the strongly localized core hole has larger dipole matrix elements with atomic-like than with bandlike wave functions. Evidence for this comes not only from multiplet calculations but also from the observed resonant enhancement in photoemission for excitation energies within the white lines.[34,35]

In a recent paper[36] we showed that for deep core levels there is a systematic change in the branching ratio with the ground-state spin-orbit energy in the atom. The largest branching ratio is obtained for the Hund's rule J level. In this paper we extend this model by taking both spin-orbit and electrostatic interactions into account for atomic and crystal-field ground states. We have performed

calculations for the branching ratios of (L,S,J) levels in atomic configurations d^n. The results can be formulated in general rules. Moreover, these atomic branching ratios can be related to those of solid-state compounds. Often, a crystal-field splitting has no or little influence on the branching ratio, except when it produces a low-spin ground state. More generally, when the ground state in the solid can be expressed in (L,S,J) or (L,S) functions the branching ratio obtained has a value which is characteristic for these atomic functions. Therefore, using the rules which will be given for the branching ratio, the spin state and total angular momentum can be assessed without actually performing crystal-field calculations.

The organization of this paper is as follows: First, we will give three basic rules which describe the variation of the atomic branching ratio in the presence of spin-orbit splitting and electrostatic interactions. Then, three additional rules are given, which are valid in the presence of a crystal field. These rules facilitate the explanation of the calculational results for the 3*d*, 4*d*, and 5*d* transition-metal compounds in the next sections. Also the rare earths are discussed. Finally, we will compare the theory with experimental data from the literature and discuss applications.

II. THEORY OF THE ATOMIC BRANCHING RATIO

In this section three rules are given, which describe the behavior of the branching ratio for purely atomic interactions. For the sake of concreteness these rules are explained with the example of the $L_{2,3}$ absorption in transition metal compounds. The white lines are due to dipole transitions from initial configurations d^n to final configurations $2p^5d^{n+1}$.

The initial state in the free atom (or ion) has definite values of L and S due to the electrostatic interactions. In the presence of a spin-orbit interaction ζ_d the initial state has also a definite value of the total atomic angular-momentum quantum number J. Crystal-field interaction is the subject of the next section.

The core-hole spin-orbit interaction ζ_p splits the final states into two p_j manifolds $(j=\frac{3}{2},\frac{1}{2})$, which are well separated in energy, except for the early 3*d* metals. Although in intermediate coupling $j=\frac{3}{2}$ and $\frac{1}{2}$ are no longer exact quantum numbers, we use them to denote the low- and high-energy manifolds, respectively. The branching ratio is defined as the intensity ratio $I(L_3)/[I(L_2)+I(L_3)]$, i.e., the fraction of the total transition probability which goes into the $2p_{3/2}$ manifold. If the Slater integrals F^2, G^1 and G^3 between the p and d electrons are not negligible compared to ζ_p, the final states have to be calculated in intermediate coupling. The largest of these Slater integrals is called $U(p,d)$.

Within this framework we can give the following three rules and their explanations.

Rule 1: In the absence of both spin-orbit coupling in the initial-state and electrostatic interactions between core-hole and valence electrons in the final state the branching ratio is statistical.

In the specific example of the $L_{2,3}$ absorption this rule states that the branching ratio is $\frac{2}{3}$ if $U(p,d)$ and ζ_d are zero. The rule can be proven rigorously,[37] even in the presence of a crystal field, using standard angular-algebra techniques.[38–40]

A detailed analysis of how nonstatistical branching ratios are produced is given with rules 2 and 3. Here we will give a short general discussion. The best way to discuss nonstatistical branching ratios is to consider the optical process as the change of a valence hole into a core hole.

There are two effects which make the two final-state manifolds different. First, there is the spin-orbit coupling of the core hole which gives the manifolds a different value of j. This difference can only influence the branching ratio when there is spin-orbit coupling in the initial state. When there is not, the spin and orbit of the hole to be excited are oriented randomly and therefore the hole can have no preference for change into either type of core hole. Second, when there are electrostatic core-valence interactions in the final state the core hole is coupled to the valence holes. The result of this coupling is different in the two manifolds. The presence of electrostatic interactions in the initial state couples the hole to be excited to the other holes in a specific way which can give it a preference for the coupling situation in one of the manifolds.

We can make the following generalization: When an interaction makes the two final-state manifolds different, then this interaction has to be present also in the initial state in order to appreciate the difference.

This analogy of spin orbit and electrostatic interactions is obscured by the fact that core-hole spin-orbit interaction is always present in the final state and we need spin-orbit interaction in the initial state to detect its effect, whereas electrostatic interactions are always present in the initial state and we need their presence in the final state to detect them.

Rule 2: High-spin states have on average a larger branching ratio than low-spin states, if spin-orbit splitting in the valence band can be neglected.

The allowed final states in XAS must have contributions of the same spin as the initial state, because only dipole transitions with $\Delta S=0$ are possible. The branching ratio will be dependent on the spin distribution over the core-hole manifolds. If $U(p,d)=0$ the character of any LS basis function in the final state is distributed statistically over the p_j manifolds. If $U(p,d)\neq 0$ the two p_j manifolds, which do not shift in energy to first order, mix in such a way that relatively more high-spin character appears in low-energy states and low-spin character in high-energy states. The reason for this is that with increasing $U(p,d)/\zeta_p$ the distribution of the spin character changes smoothly to the pure LS-coupled case with $\zeta_p=0$, where high-spin states have on the average a lower energy than low-spin states due to exchange interaction. This is shown in Fig. 1, which gives the energy distribution of the terms in the final state configurations $2p^53d^{n+1}$ in the LS coupling limit. The terms with the same S value are collected in a column for which the average energy is indicated. Despite the large energy spread, the average energy of these columns increases with decreasing values of S. The terms with the highest spin always have the lowest average energy. Because of

the nonstatistical distribution of spin character over the manifolds in intermediate coupling, together with $\Delta S=0$, a high-spin ground state has preference to dipole transitions to $p_{3/2}$ final states and a low-spin ground state to $p_{1/2}$ final states.

The process of continuous change from LS to jj coupling is illustrated in Fig. 2, where the Ni $3d^8 \rightarrow 2p^5 3d^9$ transition probability from the initial-state terms ^3F, ^1D, and ^1G is given as a function of $U(p,d)/\zeta_p$. The spectra at the top have $U(p,d)=0$ and a branching ratio equal to $\frac{2}{3}$. The bottom spectra obey LS coupling ($\zeta_p=0$) and the final states are, in order of increasing energy, ^1D, ^3F, ^3D, ^3P, ^1F, and ^1P (cf. Fig. 1). Although the term ^1D in the p^5d^9 configuration violates Hund's rule, the average energy of the triplets is still lower than that of the singlets. From a ground-state ^3F only the final states ^3D and ^3F can be reached, which are at the low-energy side. When ζ_p is increased two mechanisms can transfer intensity to the high-energy side. A level may split from ^3D or ^3F and move towards the $p_{1/2}$ region or a forbidden level with high energy mixes with ^3D or ^3F and gains intensity. Both effects are present in Fig. 2(a). The spectra of the initial states ^1D and ^1G in Figs. 2(b) and 2(c) show a similar evolution. Because in LS coupling the intensity is more at the high-energy side, the branching ratio of the singlet states in intermediate coupling is lower than that of the triplet states.

The approximate $M_{2,3}$ and $L_{2,3}$ spectra are indicated in Fig. 2(a) and it is instructive to see how the spectrum changes from LS coupling to jj coupling when one goes to ever deeper core holes. The parameter ratio for the $M_{2,3}$ spectra is close to the LS coupling limit in Fig. 1. Note that high-spin and low-spin ground states have their main peaks at quite different parts of the $M_{2,3}$ spectrum[6] and this spectrum should therefore be very sensitive to a change in the ground-state spin. In the jj coupling limit the atomic spectrum is independent from the initial state.

Another interesting feature of Fig. 2 is that it offers an interpretation of the fine structure in core-hole spectra. It is clear that the shoulders in the spectra near the jj limit are the remnants of the peaks in the LS limit. The character of, e.g., high-spin LS terms is not only distributed preferably to the $p_{3/2}$ manifold, but within each

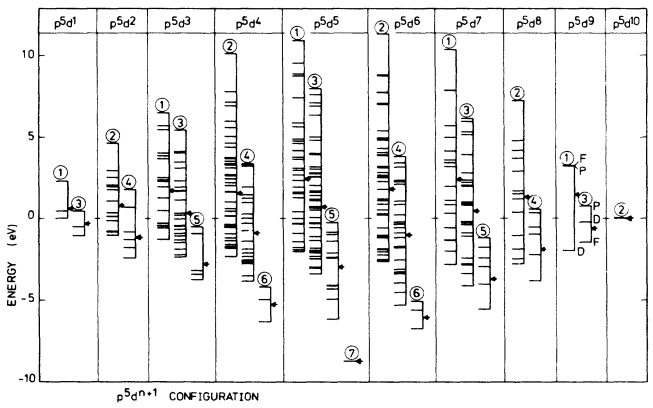

FIG. 1. Energy distribution for the terms in the final-state configurations $2p^5 3d^{n+1}$ calculated in LS coupling ($\zeta_p=0$, $\kappa=1$). The columns contain all terms with the indicated value of $2S+1$. Labels for L are only indicated in p^5d^9. The average energy of each configuration is set to zero. The arrows give the average energy of each S manifold.

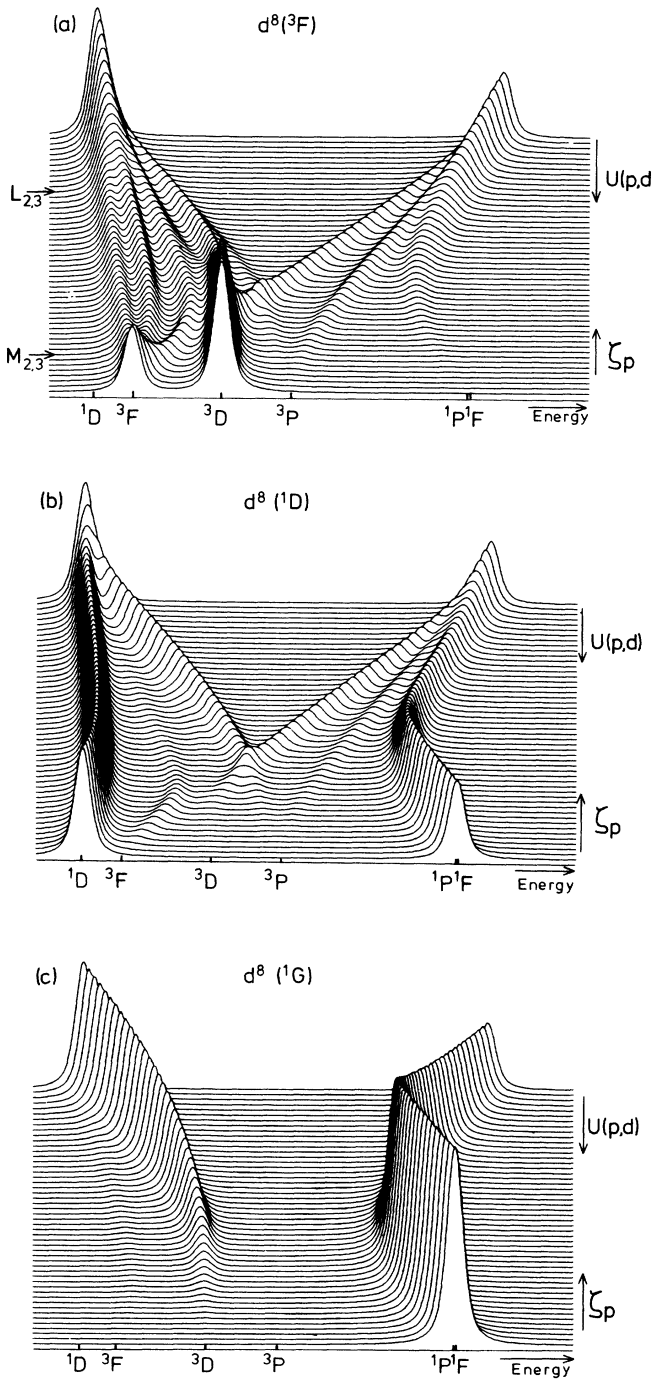

FIG. 2. Calculated transition probability of the transition $d^8 \rightarrow p^5 d^9$ for the initial states (a) ^3F, (b) ^1G, and (c) ^1D as a function of $U(p,d)/\zeta_p$. The top spectra are in jj coupling. The energy position of the final states are given for the bottom spectra in LS coupling. The approximate $M_{2,3}$ and $L_{2,3}$ absorption spectra for atomic Ni $3d^8$ are indicated.

manifold it also goes preferably to the low-energy side.

We have strongly emphasized the effect of the initial-state S value on the spectral distribution, but the same arguments also apply to L. However, the effect of L is smaller because L has less influence on the final-state energy and because the selection rule $\Delta L = 0, \pm 1$ smears out the effect on the branching ratio.

An important consequence of the $\Delta S = 0$ selection rule is the systematic change of the branching ratio along the d series. For less than half-filled shells the high-spin final state is a *ghost* spin state which cannot be reached from the initial state. This can be seen in Fig. 3 which gives the possible $2S+1$ values for the initial- and final-state configurations in LS coupling. For $n=0$ to 4 the maximum spin in the initial state is one less than in the final state, but for $n=5$ to 10 the spin space is the same in initial and final states. The high-spin ground state is effectively low spin in the final state for d^0 and d^1, and intermediate for d^2 to d^4, whereas it is really high spin for d^5 to d^8. For this reason the branching ratio increases strongly with the d count for less than half-filled shells. For more than half-filled shells there is no longer a strong change in the branching ratio, because the high-spin ground state has the highest spin possible in the final state. Because $U(p,d)/\zeta_p$ decreases with the d count the high-spin branching ratio is largest near d^5 and decreases slowly towards the end of the series. For the latter reason also the difference between high-spin and low-spin in more than half-filled shells decreases with the d count.

Rule 3: When an initial state LS term is split by spin-orbit splitting the largest branching ratio is obtained for the level $J = L \mp S$ where the negative (positive) sign is for less (more) than half-filled shells. Note that this is just the Hund's-rule ground level. For the other J levels the branching ratio gradually decreases with J. The branching ratio, averaged over all J levels of a split LS term, is equal to that of the unsplit LS term.

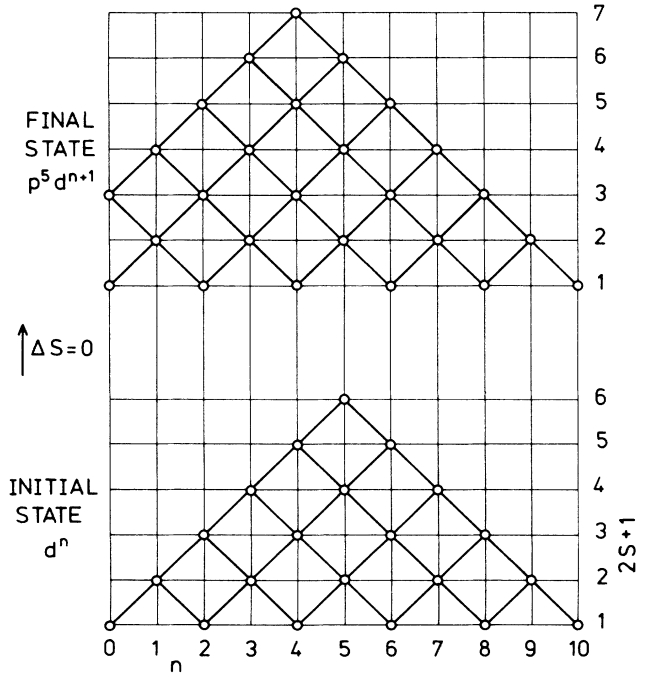

FIG. 3. Possible spin multiplicities $2S+1$ in the initial configurations d^n and final configurations p^5d^{n+1}. Because in XAS only transitions with $\Delta S=0$ are allowed, the high-spin final state for $n=0$ to 4 is a ghost spin state (see text).

This rule can also be formulated more quantitatively. If $U(p,d)=0$, it can be proven that the branching ratio for a pure ground (L,S,J) level differs from the statistical value by an amount B_1 which is proportional to the angular-algebraic part of the ground-state spin-orbit energy:

$$B_1(\alpha,L,S,J) = A(c,l,n)\frac{(E_{\alpha LSJ}-E_{\alpha LS})}{\zeta_d} , \tag{1}$$

where $(E_{\alpha LSJ}-E_{\alpha LS})$ is the well-known energy dependence on J relative to the energy of the unsplit term:[41]

$$E_{\alpha LSJ}-E_{\alpha LS} = \tfrac{1}{2}[J(J+1)-L(L+1) -S(S+1)]\zeta(\alpha,L,S) , \tag{2}$$

where $\zeta(\alpha,L,S)$ is the effective spin orbit splitting factor of the term αLS

$$\zeta(\alpha,L,S) = \frac{[l(l+1)(2l+1)]^{1/2}\langle l^n\alpha LS\|V^{(11)}\|l^n\alpha LS\rangle}{[L(L+1)(2L+1)S(S+1)(2S+1)]^{1/2}}\zeta_d \tag{3}$$

where $V^{(11)}$ in the reduced matrix element is Racah's unit double tensor operator, c and l are the core and valence-shell orbital momenta, n is the occupation number of the valence shell, α labels different terms of equal LS. The factor $A(c,l,n)$ in Eq. (1) is inversely proportional to the number of holes in the specific core-hole to valence-band transition. The value of $A(c,l,n)$ is $-(1/3)[1/(10-n)]$ for $p\rightarrow d$ transitions and $-(4/15)[1/(14-n)]$ for $d\rightarrow f$ transitions.

Equation (1) can be proven by applying standard angular momentum techniques to Cowan's line-strength formulas,[41,42] as will be published elsewhere.[37] The more qualitative formulation in rule 3 remains also correct when $U(p,d)\neq 0$ as long as it is small compared to ζ_p.

It is clear that B_1 depends only on the angular part $Z(\alpha,L,S)=\zeta(\alpha,L,S)/\zeta_d$ of the spin orbit interaction and not on its actual size which is determined by ζ_d.

The quantity $\zeta(\alpha,L,S)$ may be either positive or negative. If $\zeta(\alpha,L,S)$ is positive the term is said to be normal and then for increasing J the initial state energy increases, while the branching ratio decreases. If $\zeta(\alpha,L,S)$ is negative this is just the other way around. For less than half-filled subshells $\zeta(\alpha,L,S)$ is usually positive, especially for the lowest term of a configuration; however, negative values of $\zeta(\alpha,L,S)$ are not infrequent and the inverted structure is not by any means to be considered abnormal. For more than half-filled shells $Z(\alpha,L,S)$ has the opposite sign:

$$Z(l^{4l+2-n},\alpha,L,S) = -Z(l^n,\alpha,L,S) . \tag{4}$$

As an illustration of rule 3 Fig. 4(a) gives the calculated branching ratios with $U(p,d)=0$, in which case the term

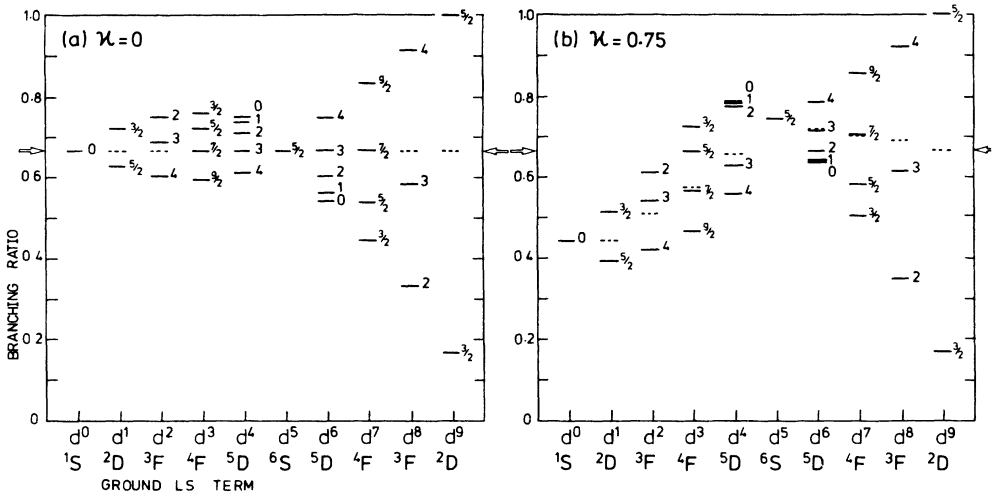

FIG. 4. Calculated branching ratios for the indicated J levels of the Hund's-rule ground LS terms in the transitions $3d^n(L,S,J)\rightarrow 2p^5 3d^{n+1}$. (a) $\kappa=0$, which is also appropriate for $4d$ and $5d$ metals; (b) $\kappa=0.75$, where κ is the scaling factor for the Slater integrals. The dashed lines give the term averaged values. The arrows on the axes indicate the statistical value.

averaged value is equal to the statistical value. The labels in the figure give the J values of the lowest LS term. The statements of rule 3 are easily verified from this figure. Because $A(c,l,n)$ is inversely proportional to the number of holes in the initial state, B_1 increases by a factor of 9 going from d^1 to d^9. The diagram for $U(p,d)\neq 0$ in Fig. 4(b) is discussed in Sec. VI B.

III. THEORY OF THE BRANCHING RATIO IN POINT-GROUP SYMMETRY

In the presence of a crystal-field interaction the initial state has definite values of ΓS, where Γ is an irreducible representation of the local point group.[43] Translational symmetry has mainly the effect that in the solid the states are broadened into bands. If the spin-orbit splitting ζ_d is large compared to the bandwidth W, the ΓS bands split into bands with different total representation Γ_J. The ground state is the lowest (Γ,S,Γ_J) level. If the band width is much larger than ζ_d the ground state is a ΓS term, i.e., all Γ_J levels are considered equally populated.

In a crystal field we have additional rules to treat the three cases: $\zeta_d=0$, ζ_d is larger than and smaller than the crystal-field interaction. The purpose of these rules is to obtain the branching ratio without performing a complicated crystal-field calculation.

Before giving the rules we will first give a general lemma. This lemma deals with a small perturbation which splits the degenerate levels of the initial and final states into sublevels belonging to irreducible representations of a subgroup of the original point group. We will use the approach exposed in Butler[44] and adopt his notation. The original intensity for a transition from a level of symmetry Γ to a final state level of symmetry Γ' using light polarized as a component of symmetry γ of the dipole operator is given by a reduced matrix element in the original point group:

$$I_{\Gamma\rightarrow\Gamma'}=\frac{1}{|\Gamma|}\,|\langle\Gamma\|C^{(1)}_{\gamma}\|\Gamma'\rangle|^2 . \tag{5}$$

The reduced matrix element in the subgroup between states $\Gamma\lambda$ and $\Gamma'\lambda'$ with dipole component $\gamma\mu$ is

$$\langle\Gamma\lambda\|C^{(1)}_{\gamma\mu}\|\Gamma'\lambda'\rangle=\langle\Gamma\|C^{(1)}_{\gamma}\|\Gamma'\rangle\begin{bmatrix}\Gamma^* \\ \lambda^*\end{bmatrix}\begin{bmatrix}\Gamma^* & \gamma & \Gamma' \\ \lambda^* & \mu & \lambda'\end{bmatrix} . \tag{6}$$

The sum over μ and λ' of the square of the $3jm$ factor (or isoscalar factor) (Ref. 44) in Eq. (6) gives $|\lambda|/|\Gamma|$ and therefore

$$\frac{1}{|\lambda|}\sum_{\mu,\lambda'}|\langle\Gamma\lambda\|C^{(1)}_{\gamma\mu}\|\Gamma'\lambda'\rangle|^2 =\frac{1}{|\Gamma|}\,|\langle\Gamma\|C^{(1)}_{\gamma}\|\Gamma'\rangle|^2 . \tag{7}$$

This equation says that the isotropic intensity in the subgroup is independent of the ground-state sublevel λ and equal to the original intensity. We have omitted branching and product multiplicities, but taking these into account we obtain the same conclusion.

Splitting lemma: If an interaction lowers the symmetry of the Hamiltonian and only one sublevel of the original ground level is populated, then if we cannot resolve the splittings in the final state, the isotropic dipole spectrum does not change.

This lemma also applies if in the final state the levels are not only split, but also mixing between these levels occurs. The mixing results in redistribution of intensity between levels within an energy range Δ, where Δ is a typical matrix element of the interaction. If the experimental resolution is larger than Δ the spectrum is unchanged. Being only interested in the branching ratio we effectively use a resolution of, say, $\zeta_p/2$. If $\Delta<\zeta_p/2$ the change of the branching ratio is of the order of Δ/ζ_p. However, if the perturbation is a crystal field, which does not act on core functions then, in the jj coupling limit, the p_j manifolds are not mixed, to first order, and the change in the branching ratio is even much less than this.

In practice for a crystal field, it is less than 2% for the $L_{2,3}$ absorption in the $3d$ transition metals.

Rule 4: If there is no valence-band spin-orbit coupling a crystal-field term has a branching ratio characteristic of the atomic terms with the same spin.

Many configurations have only one high-spin LS term. The branching ratio of a high-spin crystal-field term in those configurations is, to first order in $U(p,d)$, equal to the atomic ratio.

For some high-spin states and for all lower spin states there is more than one LS term with the same spin. The branching ratio is then generally, to first order, equal to the average of the ratios of the LS terms weighted with their character in the ground state. In order to prove this we first observe that the action of the crystal field in the final state has a negligible influence on the branching ratio. When $U(p,d)=0$ the crystal field does not mix the p_j manifolds because it does not act on the core hole. Only mixing within each manifold occurs but this cannot change the branching ratio because the sum of all intensities of a manifold is invariant to such mixing. When $U(p,d)\neq 0$ the manifolds are already mixed and then there are crystal-field matrix elements between the manifolds giving a second-order effect on the branching ratio (in practice amounting to at most 2% in the $3d$ transition metals). Thus to good approximation we may neglect the effects of the crystal field in the final state which then becomes equal to the atomic final state. Because the branching ratio is mainly determined by the distribution of spin character over the two manifolds, which is not changed by the crystal field, we may expect that a crystal-field term has a branching ratio characteristic for LS terms with the same spin.

However, in many cases we have a stronger argument for the statement that the branching ratio is approximately the average of the ratios of the LS terms: When the crystal field mixes LS terms of different L in the ground state there are no cross terms in the spectrum arising from different L's. This can be proved by angular algebra techniques.[38] The absence of cross terms means that the spectrum is exactly the average of the spectra of the different LS terms, weighted by their character in the ground state. In high-spin states there is always only one term of each L but, e.g., for d^3 to d^7 there are LS terms of intermediate and low spin occurring more than once. If more than one term with the same LS has significant character in the ground state there may be cross terms changing the spectrum and the branching ratio and then our arguments are no longer exact.

Rule 5: In a crystal field which is smaller than the valence-band spin-orbit coupling an atomic (L,S,J) level splits into (L,S,J,Γ) states which all have the branching ratio of the (L,S,J) level.

This is a direct consequence of our splitting lemma. It applies especially to the rare earths. It is not possible to detect crystal-field effects in rare-earth materials by measuring the isotropic branching ratio. Polarization-dependent spectra can give information on the crystal field, but only in symmetries other than octahedral or tetrahedral.

Rule 6: When an initial-state crystal-field term ΓS is split into levels (Γ,S,Γ_J) by a spin-orbit splitting which is small compared to the crystal field, each level has a different branching ratio, decreasing with increasing energy.

This rule is an extension of rule 3 and it can be proved in a similar way. More precisely, the change in the branching ratio is proportional to the angular algebraic part of the first order energy splitting, with the same proportionality constant $A(c,l,n)$. Levels which are split or shifted in second order also have a different branching ratio, but this effect is small and is best determined by a complete crystal-field calculation.

Often the spin-orbit coupling is quenched, which means that the first-order effect is zero by symmetry. The following prescription may be used to determine which ΓS terms split to first order: Split S into point-group representations Γ_S and split the momentum 1 of the operators s and l from the spin-orbit interaction $\mathbf{s}\cdot\mathbf{l}$ into representations γ. Inversion symmetry must be disregarded and Kramers pairs must be considered as one degenerate representation. The necessary conditions are then as follows: (1) The set of all Kronecker products $\Gamma_s\times\Gamma$ consists of more than one irreducible representation (counting repetitions). (2) $\Gamma\times\Gamma$ and $\Gamma_s\times\Gamma_s$ have at least one of the γ in common. Condition 2 is met by all degenerate representations of all point groups except the (two-dimensional) E representation of O and T_d. In the groups C_s, C_n, C_{nh}, and S_{2n} the set of γ contains the totally symmetric representation and then condition 2 is met for all terms.

In the following we will apply the branching ratio rules to transition metals and rare earths, taking into consideration the conditions for which each rule is valid. When in $3d$ transition metals the spin-orbit splitting is quenched or it is less than the bandwidth, the branching ratio is determined by the spin state (rule 4). If in $3d$, $4d$, and $5d$ transition metals ζ_d is small compared to the crystal field, the ΓS terms split into levels, each with a different branching ratio (rule 6). In the rare earths the crystal field is smaller than ζ_{4f}. The crystal-field splitting of (L,S,J) levels into (L,S,J,Γ) levels does not change the branching ratio (rule 5).

IV. CALCULATIONAL DETAILS

The branching ratio of the LS terms and (L,S,J) levels for the transition metals were calculated using Cowan's computer code for atomic radiative transitions.[41,42] In these calculations the dipole transition probabilities are obtained from a Hartree-Fock program to determine the initial- and final-state wave functions and energies. The line strengths obtained were summed separately for the two manifolds. The point of separation between the manifolds was chosen such that their variances were as close as possible. For well-separated manifolds this point is in the gap. When there is no clear separation the choice becomes more or less arbitrary. This occurs in the early $3d$ metals for large electrostatic interactions, cf. Sec. VI A.

The free-ion values of the Coulomb and exchange integrals have to be scaled by a factor κ which takes into

account effects such as atomic correlation and covalent mixing.[45] Comparison of detailed multiplet calculations with experimental spectra shows that κ is usually about 0.75,[16,33] although compound-dependent values for transition metals have been reported between 0.4 and 1.[5,6,46,47]

The calculations in crystal-field symmetry were performed using the chain of groups approach exposed by Butler.[44] The reduced matrix elements of the operators obtained with Cowan's computer code, are transformed to the required point group, using the Wigner-Eckart theorem. The isoscalar factors were calculated with Butler's point-group program, which uses modern group-theoretical results[48] to obtain a consistent set of coefficients for all groups.

V. THE $L_{2,3}$ ABSORPTION IN 4d AND 5d TRANSITION-METAL COMPOUNDS

A. Atomic calculations

The value of $U(p,d)/\zeta_{2p}$ in the 4d and 5d metals is ~ 0.02 and ~ 0.002, respectively. Therefore, these transition-metal atoms can be treated in the limit of jj coupling and the atomic branching ratio can be calculated straightforwardly using Eq. (1). The spin-orbit parameter ζ_d varies in the 4d metals from ~ 0.03 to ~ 0.2 eV and in the 5d metals from ~ 0.1 to ~ 0.5 eV. The branching ratios for the J levels of the pure Hund's-rule ground terms are given in Fig. 4(a). The regularity in the spacing can be disturbed because L and S are not always good quantum numbers in the presence of spin-orbit coupling. A calculation for the branching ratios in 4d transition-metal atoms which does take this second-order spin-orbit interaction with higher LS terms into account can be found in Ref. 36.

The ground terms have a normal sequence of the J levels: the branching ratio is increasing (decreasing) for higher J for more (less) than half-filled shells. Some high-energy LS terms have an inverted sequence because $\zeta(\alpha,L,S)$ is negative, but this occurs only in the ^2F and second ^2D terms of d^3 and d^7 and in the ^3D, second ^3F, and second ^3P terms of d^4 and d^6.

B. Crystal field

Except for the heaviest 5d metal compounds, ζ_d is usually smaller than the crystal field and rule 6 applies. The branching ratio can be obtained from Eq. (1) with the energy difference calculated in the proper point-group symmetry, although we used the procedure outlined in Sec. IV. We give here only the results for the high-spin states in a crystal field of octahedral symmetry. In first order only the terms with orbital symmetry T_1 and T_2 are split by ζ_d. In second order the other terms can also be split or can undergo a shift in energy. The branching ratios for all Γ_J levels of the ground terms ΓS are shown in Fig. 5(a). Because $\kappa=0$ the average over Γ_J is equal to the statistical value, except for a small shift caused by the second-order spin-orbit interaction. The variations of the branching ratio for the (Γ,S,Γ_J) levels are about the same as those for the atomic (L,S,J) levels, except when the spin orbit interaction is quenched. The level Γ_J with the lowest energy has the highest branching ratio. The second-order effects in Fig. 5(a) must be considered as only illustrative, because they depend on, e.g., $10Dq$.

VI. THE $L_{2,3}$ ABSORPTION IN 3d TRANSITION-METAL COMPOUNDS

The 3d transition metals are more complicated than the 4d and 5d metals because 2p-3d electrostatic interactions are important in the final state. In the 3d transition metals ζ_{2p} changes from 2.4 in Ca to 11.5 eV in Ni, whereas $U(2p,3d)$ changes from 3.8 to 7.7 eV. Therefore, $U(2p,3d)/\zeta_{2p}$ decreases in the 3d series from 1.58 to 0.67. We will first give the results in the absence of 3d

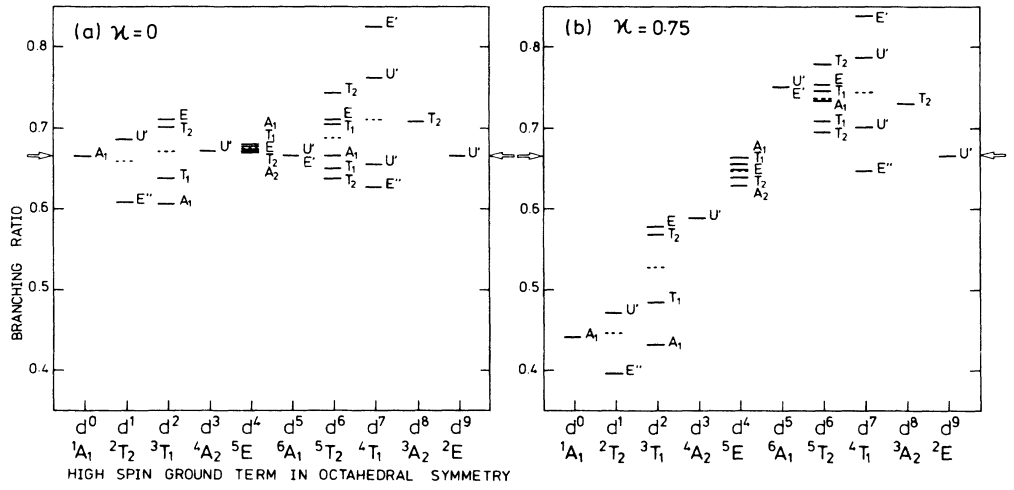

FIG. 5. Calculated branching ratios for the Γ_J levels of the high-spin ground terms in octahedral symmetry in the transitions $3d^n(\Gamma,S,\Gamma_J)\rightarrow 2p^5 3d^{n+1}$. (a) $\kappa=0$; (b) $\kappa=0.75$. The dashed lines give the term-averaged values. The arrows on the axes indicate the statistical value.

spin-orbit splitting and crystal field, in which case rule 2 holds.

A. $\zeta_d = 0$

The diagrams in Fig. 6 give the calculated branching ratios of all possible LS terms in the $3d^n$ configurations as a function of κ. The limit of pure jj coupling is given by $\kappa = 0$ and the situation with unscaled atomic Slater integrals by $\kappa = 1$. The relevant region for κ is between 0.4 and 1, depending on the covalent mixing in the compound, although κ is most often around 0.75 to 0.8.

As is also expected from rule 1 the branching ratio at $\kappa = 0$ is always statistical. For nonzero κ the branching ratio changes as described by rule 2. This change is linear for small values of κ, but at larger values the branching ratios change more abruptly because the two p_j manifolds start to penetrate each other. As seen in Fig. 6 the value of κ for which this occurs increases along the d series, because the Hartree-Fock value of $U(2p,3d)/\zeta_{2p}$ gradually decreases along the $3d$ series.

High-spin states have on the average a larger branching ratio than low-spin states. This enables us to identify the spectra of many high- and low-spin compounds at first sight by their extreme branching ratios, even if the value of κ is not precisely known. For intermediate-spin and low-spin compounds the ranges of possible branching ratios have some overlap, which makes their distinction less clear.

The highest branching ratio within a configuration is obtained for the Hund's-rule ground term. Subsequently lower branching ratios are found for terms with higher energy. This can be checked from Fig. 7, which gives the energy of all the terms in the initial configurations $3d^n$. Comparing the branching ratios of Fig. 6 for not-too-large values of κ and the energy diagrams of Fig. 7, where the energy axis has been inverted, there is an overall agreement in the sequence in which the terms appear, although there are quite a few permutations in the middle of the diagram. The physical reason for this resemblance is that energy and branching ratio are both determined by electrostatic interactions, although the energy is determined by d-d interactions and the branching ratio by p-d interactions. It is interesting that an even more striking resemblance exists between the branching ratio sequence for d^n and d^{10-n}. The origin of this resemblance is not clear.

So far we have only discussed the changes in branching ratios within the individual configurations. An important consequence of the $\Delta S = 0$ selection rule is the systematic change along the d series. For less than half-filled d shells the *ghost* spins in the final state (cf. Fig. 3) clearly manifest themselves by the absence of higher-than-statistical branching ratios. Figure 6 shows that the branching ratios of all terms in d^0 to d^3 are decreasing with increasing κ. For larger d count this is no longer

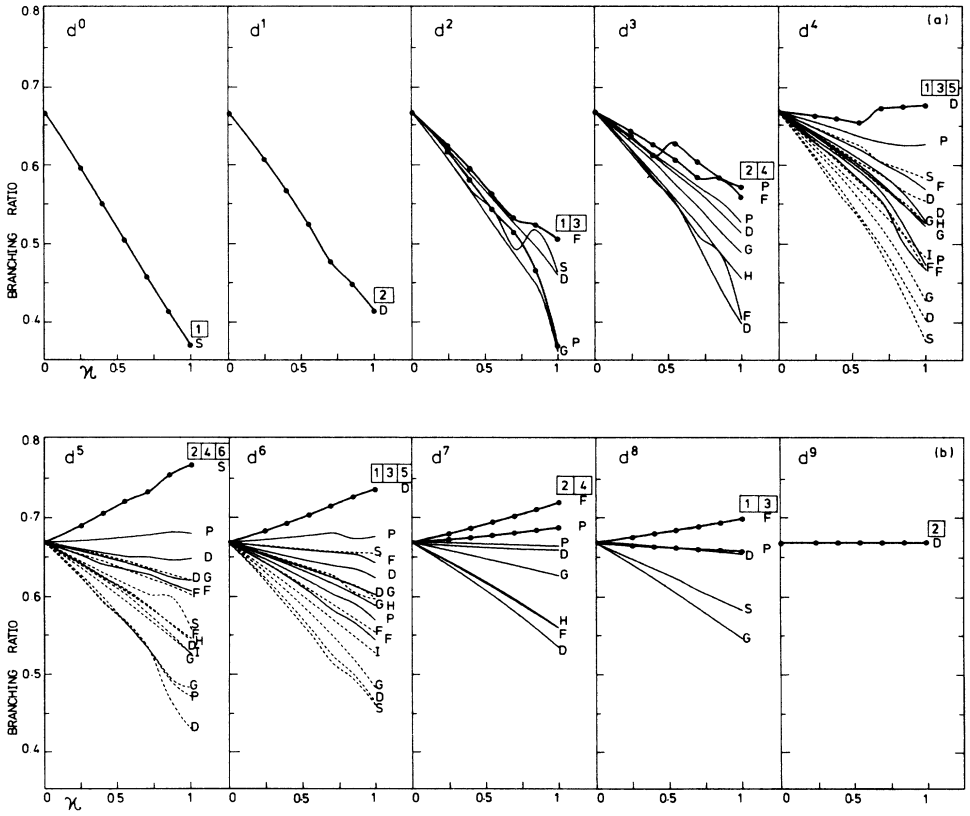

FIG. 6. The $L_{2,3}$ branching ratio diagrams for all terms in the $3d$ transition metal atoms as a function of κ. (a) d^0 to d^4, (b) d^5 to d^9. The curves for high-spin and subsequently lower-spin terms are thick float lines (——), thin lines, and dashed lines, respectively. The columns with the L values of the terms are labeled by the corresponding $2S+1$ value.

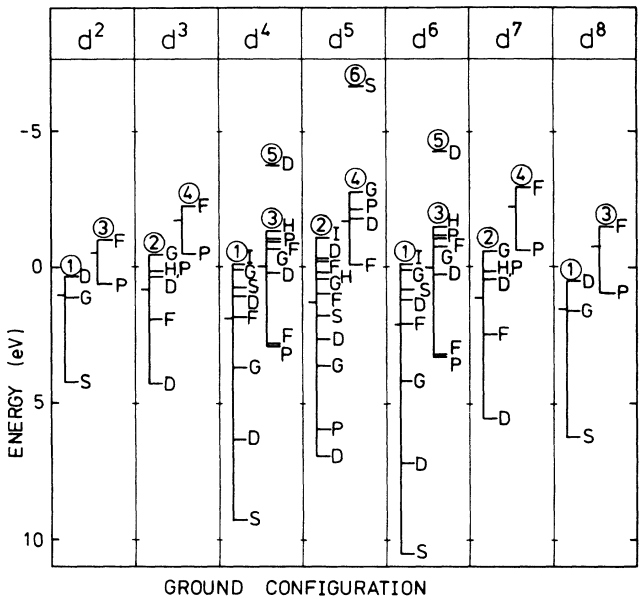

FIG. 7. Energy distribution of the terms in the initial-state configurations $3d^n$ ($\kappa=1$). The terms are collected in spin manifolds, where the labels give the values of $2S+1$ and L. The average energy of the configuration is set to zero and the average energy of each spin manifold is indicated. The energy axis has been inverted for the ease of comparison with Fig. 6.

true. The high-spin terms in d^5 to d^8 have a branching ratio larger than or about equal to the statistical value. The only exception is the ^3P term in d^8, where transitions can only take place to the final-state terms ^3P and ^3D, which have relatively a high energy (see Fig. 1). For d^9 the branching ratio remains statistical due to the absence of p-d interactions in the final state.

B. $\zeta_d \neq 0$

The $3d$ spin-orbit parameter increases in the first row series from ~ 0.01 to ~ 0.1 eV and cannot always be neglected. From Fig. 4(a) with $U(p,d)=0$ it was already clear that ζ_d has a substantial influence on the branching ratio. For the $3d$ metals we must also consider the $2p$-$3d$ interactions.

The calculated branching ratios in the presence of Coulomb and exchange integrals ($\kappa=0.75$) are given in Fig. 4(b) for all J levels of the ground LS terms. Also for each LS term the weighted average over J is given. This value is no longer equal to the statistical value but equal to the value in Fig. 6. It is clear from comparison of Figs. 4(a) and 4(b) that electrostatic interactions shift the term averaged values by a large amount but that the mutual distances between the J levels in a given LS term remain globally the same. Only the levels $J=0$ and 1 in the ^5D term of d^6 cross each other at $\kappa=-0.85$.

In Fig. 4(b) we see again the systematic trend along the series which is a consequence of both the selection rule $\Delta S=0$ and the gradual decrease in $U(2p,3d)/\zeta_{2p}$. The deviation from the statistical value for the term-averaged branching ratio is largest for the lower d counts. As seen the term-averaged value increases strongly from below the statistical value in d^0 to above the statistical value in d^5. From this maximum it returns slowly to the statistical value in d^9. We see that in the absence of spin-orbit interaction the branching ratio can be used as a measure for the d count, especially for less than half-filled shells. On the other hand, the branching ratio for the Hund's-rule ground-state J level increases over the whole series to a value of 1 for d^9 with a small dip for d^5. The influence of ζ_d is most pronounced for higher d counts due to the factor $A(c,l,n)$ in Eq. (1). Generally, we can say that the effect of the electrostatic interactions is most prominent for low d counts, whereas the effect of spin-orbit interaction is most pronounced for high d counts.

The non-ground-state LS terms show a similar behavior. The branching ratio of a particular (L,S,J) level can approximately be obtained by taking the average value for the LS term from Fig. 6 and by calculating for the J level the deviation from this average value using Eq. (1).

C. Crystal field

The crystal-field interaction in $3d$ metal compounds is usually larger than the ζ_{3d} spin-orbit interaction. For the high-spin terms ΓS in an octahedral crystal field we have calculated the branching ratio for all levels Γ_J. The results in Fig. 5(b) for $\kappa=0.75$ can be compared with those in Fig. 5(a) for $\kappa=0$. It is clear that the distances between the (Γ,S,Γ_J) levels in a given configuration remain globally the same. The trend of the branching ratio along the d series still resembles the atomic trend [Fig. 4(b)], except when the spin-orbit interaction is quenched by the crystal field.

Except for d^2, d^3, d^7, and d^8, every configuration has only one high-spin term. A crystal field cannot mix this term with other terms and its branching ratio will stay at the atomic value [Fig. 4(b)]. If there are more atomic terms with high spin, which do not differ too much in energy, these states will mix in the presence of a crystal field and the branching ratio obtains an average value. Low-spin states are always a mixture of low-spin LS terms and have the low branching ratio characteristic of these terms.

VII. THE $M_{4,5}$ ABSORPTION IN RARE-EARTH COMPOUNDS

For the $M_{4,5}$ absorption spectra of the rare earths, which originate from transitions $3d \rightarrow 4f$, the value of $U(3d,4f)/\zeta_{3d}$ changes from 0.83 in La to 0.51 in Tm.[16] Almost all rare-earth compounds have a ground state with an extreme J value according to Hund's third rule, because the $4f$ bandwidth is much smaller than ζ_f, which changes from 0.092 eV in La to 0.371 eV in Tm. Then, according to rule 5 the branching ratio in the solid will have the same value as in the atom. From rule 3 we know that the branching ratio will have the largest value.

The calculated atomic values for the M_4 and M_5 intensities have been tabulated in Ref. 16. The branching ratio of the ground-state J level gradually increases along the $4f$ series from 0.39 to 1, with a small dip for the $4f^7$

configuration. This trend along the rare-earth series is very similar to the trend in the $3d$ transition metals in Fig. 4(b) and the explanation is the same. The strong dependence of the branching ratio on the f count can be used to identify heterogeneous mixed-valent materials.[49,50]

Because the $4f$ electrons in rare-earth materials are highly localized, the chemical shift in the x-ray absorption lines is small.[51] This permits determination of the energy of the final states, which can be reached from the high-spin ground state with the selection rule $\Delta S=0$. The relative energy of these final states within the manifolds reflects the energy positions in the LS coupling limit as explained with rule 2. Therefore, for the La^{3+}, Ce^{3+}, and Pr^{3+} ions which are effectively low spin in the final state, the absorption lines are located at the high-energy sides of the manifolds. This results in XAS in an energy shift 2–3 eV compared with x-ray photoemission spectroscopy (XPS),[52,53] where there are no *ghost* spin states. Moreover, XPS has a less stringent selection rule, namely $\Delta S=\pm\frac{1}{2}$, and therefore more allowed final-state terms. For the heavy rare earths the XAS lines are on the low-energy sides of the manifolds. Although also in transition metals this effect is present, it is overshadowed by the large chemical shift due to the d electrons, which are participating in the bonding orbitals.

VIII. COMPARISON WITH EXPERIMENTAL RESULTS

A first question to address is how pronounced the white lines are compared to the continuum. For the transitions to the continuum states above the $L_{2,3}$ edges the cross-section varies from 2.1 Mb/atom in Sc to 1.1 Mb/atom in Cu.[54] Calculation of the total integrated cross section of the $2p\rightarrow 3d$ transitions in the $3d$ series gives a value of $16(10-n)$ Mb eV/atom, where $(10-n)$ is the number of vacancies in the $3d$ shell. The width of the white lines is determined by the intrinsic width of the $2p$ core level which is smaller than 1 eV and by the electrostatic interactions which are in the order of a few eV. Therefore, the white lines can easily be distinguished from the continuum above the edge, but most clearly for lower d counts.

This does not always mean that it is completely trivial to obtain accurate experimental values for the branching ratio. The background correction of the spectrum and the transmission function of the monochromator are obvious problems. In the early $3d$ metals there is some overlap between the two manifolds and the separation is somewhat arbitrary. Furthermore, the $p_{1/2}$ manifold is broader than the $p_{3/2}$ manifold due to Koster-Kronig transitions[55,56] and sometimes there is loss of main line intensity into satellite structures.[47,52]

We will now compare our results with available data from the literature. For $4d$ and $5d$ transition-metal compounds nonstatistical branching ratios have been observed at the end of the series, such as in Rh, Pd, Ir, and Pt compounds,[1,17,18,24,58] and the $L_{2,3}$ branching ratio for the heavier $5d$ metals has been reported as being gradually increasing with the d count.[20] This behavior is expected from Eq. (1), which predicts that the deviations from the statistical value along the series are inversely proportional to the number of holes. The influence of the initial-state spin-orbit splitting is best observed in d^9, where the level $J=\frac{5}{2}$ does not contribute to the L_2 edge. Especially Pt compounds have been well studied for this reason.[59]

The experimental $M_{4,5}$ absorption spectra of rare-earth metals[7,8,16] and compounds[60] nicely demonstrate the theory by the gradual increase in branching ratio, which is characteristic for the Hund's-rule ground-state J level. The value of the branching ratio is usually compound independent, because the ground state remains the same. Only for Ce_5Pd_{95} is a lower branching ratio than for pure Ce metal found, which accompanies an admixture of $4f_{7/2}$ character in the predominantly $4f_{5/2}$ ground state of the diluted alloy.[61] The amount of mixing in the ground state can be determined in this way.

More variation is found in the $3d$ transition-metal compounds.[33,62–64] The experimental values for the branching ratios of the oxides[11–14] are reproduced in Fig. 8. The values for Cr_2O_3 (d^3), FeO (d^6), NiO (d^8), and CuO (d^9) from Sparrow *et al.*[13] are systematically lower than those reported by Leapman *et al.*[12] (cf. Fig. 8). Except for CuO, the $3d$ transition-metal monoxides, sesquioxides, and dioxides have octahedrally coordinated metal ions with a slight trigonal distortion in the corundum structure of the sesquioxides and a slight tetragonal distortion in the rutile structure of the dioxides. The oxides all have high spin.

In Fig. 8 we also give four curves for the high-spin term, which have been taken from Figs. 4(b) and 5(b). The upper curve a gives the branching ratio for the ground-state level (L,S,J) in the atom. Curve b gives the

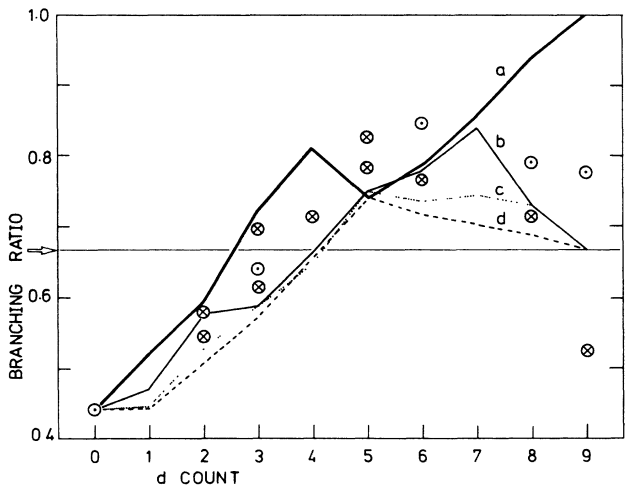

FIG. 8. Diagram giving the branching ratio of the high-spin ground state of $3d$ metal compounds in octahedral symmetry ($\kappa=0.75$). Curve a, $\zeta_{3d}>10Dq$ and W; curve b, $10Dq>\zeta_{3d}>W$; curve c, $10Dq>W>\zeta_{3d}$; and curve d; $W>10Dq$ and ζ_{3d}. The arrow points to the statistical value. Experimental data for mono-, di-, and sesquioxides from Leapman, Ref. 12 (⊙) and Sparrow, Ref. 13 (⊗).

branching ratio for the ground-state level (Γ, S, Γ_J) in octahedral symmetry. Curves c and d give the average branching ratio for the ground state LS term and ΓS term, respectively. These curves represent different situations for the crystal field and the spin-orbit interaction. Curve a gives the situation that the spin orbit parameter is larger than the crystal-field parameter and larger than the bandwidth: $\zeta_d > 10Dq$ and W. This is the maximum obtainable branching ratio as a function of the d count. High-spin octahedral compounds are expected to follow curve b, if $10Dq > \zeta_d > W$. But if W increases, the branching ratio will move towards curve c, where $10Dq > W > \zeta_d$, and finally to curve d, where $W > 10Dq > \zeta_d$. Comparison with the experimental data shows that the overall agreement is good in view of the large experimental uncertainty at the end of the series and considering that we treated all compounds in a theoretically uniform way, regardless of all chemical differences. The only free parameter κ has been set to 0.75. To first approximation a change in κ will give a proportional change in the branching ratio relative to the statistical value.

For the experimental spectra of high-spin compounds from Matsukawa and Obashi given in Yamaguchi's paper[5] and of the fluorides given by Nakai[46] a similar trend as for the oxides is observed. Only for MnF_2 and CrF_3,[46] where the experimental $L_{2,3}$ spectrum is in disagreement with calculated multiplet structure, is the experimental branching ratio lower than theoretically expected. The high-spin Ni d^8 compounds are discussed in Sec. IX.

Even for the pure metals the trend in the branching ratio is similar to the general observed trend. It strongly increases from Ca to Fe and slowly decreases from Fe to Cu.[12,26] This indicates that despite the large bandwidths and the itinerant nature of the d electrons the white lines are mainly determined by atomiclike transitions.

It is also interesting to compare directly the branching ratio of one particular absorption edge in different compounds. Experimental influences can then be reduced by measuring with constant monochromator settings. For magnetic materials such studies have established a relation between the branching ratio and the local magnetic moment. Morrison *et al.*[21] have measured the Fe $L_{2,3}$ absorption edge in various Fe_xGe_{1-x} alloys. They find that the decrease of the iron magnetic moment on alloying with germanium is accompanied by a decrease in the branching ratio. Pease *et al.*[23] found that the branching ratio for the high-spin Cr alloy $Cr_{20}Au_{80}$ is larger than for Cr metal. Morrison *et al.*[22] found that in amorphous $Fe_{30}Y_{70}$ the branching ratio is lower than in Fe metal, which accompanies a decreased magnetic moment in the alloy.

Another application is the electronic structure of diluted alloys, where the impurity atoms have a small bandwidth. Fuggle[65] finds for Ni impurities in Pd and Cu a larger branching ratio than for Ni metal, indicating an increased amount of $d_{5/2}$ character in the ground state of diluted alloys.

Also high-spin and low-spin compounds can be distinguished. In Fig. 9 we reproduce the Fe $L_{2,3}$ absorption edges of iron metal and various insulating iron compounds, such as pyrite (FeS_2), magnetite (Fe_3O_4), holmium iron garnet ($Ho_3Fe_5O_{12}$), and hematite (α-Fe_2O_3).[66] These materials have been measured using a high-resolution monochromator based on the combination of acid phthalate (AP) crystals and multilayer reflecting coatings.[67] The iron atoms in the measured compounds have configurations which differ in d count, crystal field and spin state. Only FeS_2 has a low-spin configuration and as seen the branching ratio is much smaller than in the other compounds.

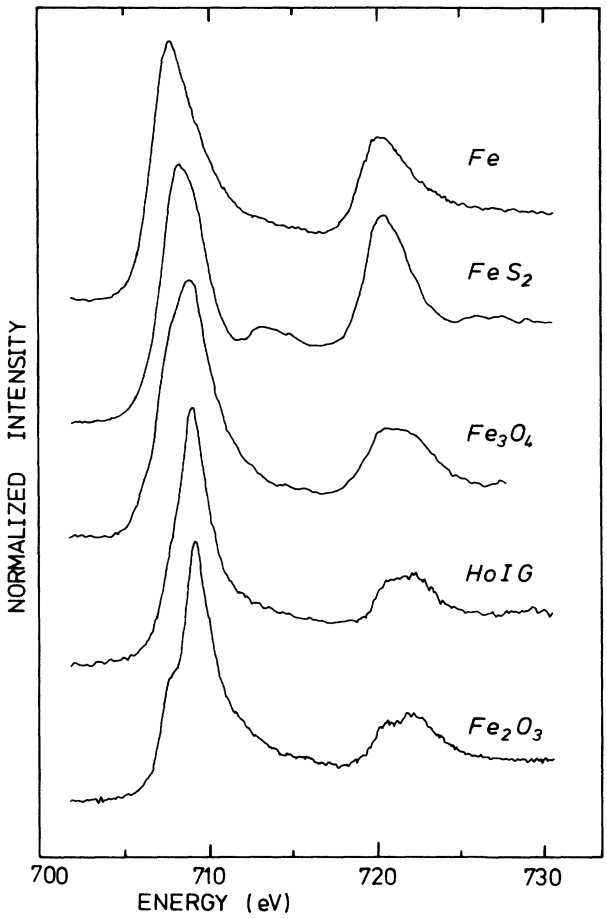

FIG. 9. Experimental Fe $L_{2,3}$ absorption spectra for different iron compounds.

IX. AN EXAMPLE: DIVALENT NICKEL

We will give an example of a spectral analysis where the combination of the branching ratio theory with detailed multiplet calculations helped us to determine the ground state of a compound. Figure 10 shows the experimental Ni $L_{2,3}$ absorption spectrum of Ni oxalate[68] with a branching ratio of 0.73. This large value indicates a high-spin compound. For low-spin compounds branching ratios around 0.6 are expected and observed.[68,69] The lines in Figs. 10(a) and 10(b) give two different multiplet

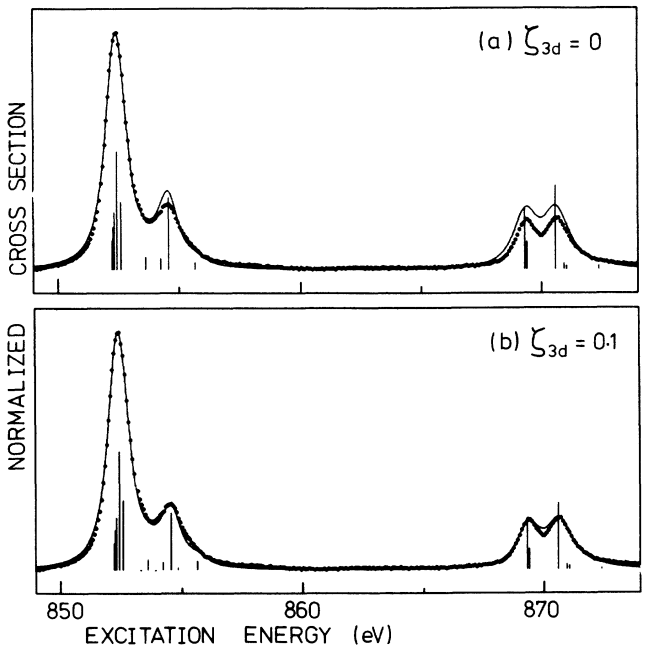

FIG. 10. Experimental Ni $L_{2,3}$ absorption spectrum for the high-spin compound Ni oxalate (dots) together with two multiplet calculations (drawn lines); (a) $\zeta_d = 0$, (b) $\zeta_d = 0.1$ eV. See text for calculational details.

calculations with $\zeta_{3d} = 0$ and 0.1 eV, respectively. The oscillator strength is calculated for transitions from the $e_g^2({}^3A_2)$ ground state in octahedral symmetry using $\kappa = 0.85$ and $10Dq = 1.5$ eV.[68] Convolution by a Gaussian of $\sigma = 0.15$ eV and a Lorentzian with $2\Gamma = 0.80$ (1.10) eV for the L_3 (L_2) accounts for the experimental broadening and the intrinsic linewidth, respectively. Figure 10(a) gives the best fit obtainable with $\zeta_{3d} = 0$. A main error is the low value of the branching ratio. This suggested that there are spin-orbit effects in the ground state even though ${}^3A_2$ does not split. In second order the term $(t_{2g}e_g\,{}^3T_2)T_2$ mixes into the ground state with a coefficient equal to $\zeta_{3d}\sqrt{2}/10Dq$. It was to be expected that $\zeta_{3d} \neq 0$ would increase the branching ratio because in the limit $\zeta_{3d} \gg 10Dq$ the value of 0.92 as for ${}^3F_4$ would be obtained (cf. Fig. 8). Indeed, the calculation including spin-orbit interaction in Fig. 10(b) gives not only the correct branching ratio but also a better agreement with the fine structure, especially for the high-energy peak in the L_3 edge. The theoretical branching ratio with $\zeta_{3d} = 0$ and 0.1 eV is 0.692 and 0.732, respectively ($\kappa = 0.85$). This increase in the $I(L_3)/I(L_2)$ ratio of 20% demonstrates the extreme sensitivity for small spin-orbit effects in the ground state.

Also for NiO and Ni dihalides,[47] where the value of κ changes with the covalent mixing, the presence of the second-order spin-orbit interaction can be seen from the branching ratio as well as from the relative intensity of the high-energy peak in the L_3 edge.

X. CONCLUSIONS

We have shown that study of the branching ratio in XAS offers a potential method to distinguish ground states of different spin and different total angular momentum in transition-metal compounds. The branching ratio is determined by the electrostatic interaction between core-hole and valence electrons and the initial-state spin-orbit splitting. For a deep core hole the final state can be described in jj coupling and the deviation of the branching ratio from the statistical value is proportional to the initial-state spin-orbit energy. This is the situation for the $L_{2,3}$ spectra of $4d$ and $5d$ metals.

In $3d$ and $4f$ metals final state electrostatic interactions are also important. For the free ion the Hund's-rule LS term has the highest branching ratio due to the electrostatic interactions. In this LS term the Hund's-rule (L,S,J) level has the highest branching ratio due to spin-orbit interactions.

A crystal field has little influence on the branching ratio, except that it has the possibility of producing a low-spin ground state, composed of one or more low-spin LS terms, with the relatively low branching ratio characteristic of these terms. Furthermore a crystal field can, partly or completely, quench the spin-orbit splitting and thereby its effect on the branching ratio. Analysis of experimental spectra using these simple considerations, together with our diagrams of free-atom data (Fig. 6) gives important information on the ground state without the necessity of doing a complete crystal-field calculation.

The model is strictly valid only for compounds with localized valence electrons. Although in metals the trend in the branching ratio is similar to the one obtained in the localized description, we believe that for materials where the valence electrons are delocalized or where configuration interaction is important more theoretical work is necessary. Even if the bandwidth is large, values of the branching ratio in a series of compounds can be compared and can yield magnetism-related information.[21–23] We expect that the branching ratio is often one of the simplest and most direct indicators for the spin of the ground state and in narrow band materials also for the spin-orbit splitting.

The value of the spin-orbit splitting in narrow-band materials may be determined by temperature-dependent branching-ratio measurements. Experimental width and core-hole lifetime broadening play no role; the branching ratio is only sensitive to broadening due to interactions in the ground state. As long as the spin of the ground state is not changed, the effects of crystal and magnetic fields on the branching ratio is often small and can moreover only be obtained by nonisotropic measurements using polarized light,[70–72] for which we do not give simple rules. Nevertheless, from the calculated magnetic x-ray dichroism (MXD) spectra of the rare earths[73] it can be seen that such measurements may in some cases by interesting.

The low sampling depth in XAS (Ref. 74) makes the branching-ratio analysis also suited to detect surface phenomena, such as surface magnetic, geometric and electronic properties different from the bulk.

*Present address: Interdisciplinary Research Centre in Surface Science, Daresbury Laboratory, Warrington WA4 4AD, United Kingdom.

[1]M. Brown, R. E. Peierls, and E. A. Stern, Phys. Rev. B **15**, 738 (1977).

[2]P. S. P. Wei and F. W. Lytle, Phys. Rev. B **19**, 679 (1979).

[3]B. Sonntag, J. Phys. (Paris) Colloq. **47**, C4-9 (1978).

[4]L. C. Davis and L. A. Feldkamp, Solid State Commun. **19**, 413 (1976); L. C. Davis, J. Appl. Phys. **59**, R25 (1987).

[5]T. Yamaguchi, S. Shibuya, S. Suga, and S. Shin, J. Phys. C **15**, 2641 (1982).

[6]S. Shin, S. Suga, M. Taniguchi, H. Kanzaki, S. Shibuya, and T. Yamaguchi, J. Phys. Soc. Jpn. **51**, 906 (1982).

[7]V. F. Demekhin, Fiz. Tverd. Tela (Leningrad) **16**, 1020 (1974) [Sov. Phys.—Solid State **16**, 659 (1974)].

[8]J. Sugar, Phys. Rev. A **6**, 1764 (1972); Phys. Rev. B **5**, 1785 (1972).

[9]A. F. Starace, Phys. Rev. B **5**, 1773 (1972).

[10]J. A. Horsley, J. Chem. Phys. **76**, 1451 (1982).

[11]R. D. Leapman and L. A. Grunes, Phys. Rev. Lett. **45**, 397 (1980).

[12]R. D. Leapman, L. A. Grunes, and P. L. Fejes, Phys. Rev. B **26**, 614 (1982).

[13]T. G. Sparrow, B. G. Williams, C. N. R. Rao, and J. M. Thomas, Chem. Phys. Lett. **108**, 547 (1984).

[14]C. N. R. Rao, J. M. Thomas, B. G. Williams, and T. G. Sparrow, J. Phys. Chem. **88**, 5769 (1984).

[15]G. Wendin, Phys. Rev. Lett. **53**, 724 (1984).

[16]B. T. Thole, G. van der Laan, J. C. Fuggle, G. A. Sawatzky, R. C. Karnatak, and J. M. Esteva, Phys. Rev. B **32**, 5107 (1985).

[17]Y. Cauchois and I. Manescu, C. R. Acad. Sci. **210**, 172 (1940).

[18]T. K. Sham, Phys. Rev. B **31**, 1888; 1903 (1985).

[19]T. K. Sham, Solid State Commun. **64**, 1103 (1987).

[20]B. Qi, I. Perez, P. H. Ansari, F. Lu, and M. Croft, Phys. Rev. B **36**, 2972 (1987).

[21]T. I. Morrison, M. B. Brodsky, N. J. Zaluzec, and L. R. Sill, Phys. Rev. B **32**, 3107 (1985).

[22]T. I. Morrison, C. L. Foiles, D. M. Pease, and N. J. Zaluzec, Phys. Rev. B **36**, 3739 (1987).

[23]D. M. Pease, S. D. Bader, M. B. Brodsky, J. I. Budnick, T. I. Morrison, and N. J. Zaluzec, Phys. Lett. A **114**, 491 (1986).

[24]N. F. Mott, Proc. Phys. Soc. London, Sect. A **62**, 416 (1949).

[25]L. F. Mattheiss and R. E. Dietz, Phys. Rev. B **22**, 1663 (1980).

[26]J. Fink, Th. Müller-Heinzerling, B. Scheerer, W. Speier, F. U. Hillebrecht, J. C. Fuggle, J. Zaanen, and G. A. Sawatzky, Phys. Rev. B **32**, 4899 (1985).

[27]Y. Onodera and Y. Toyozawa, J. Phys. Soc. Jpn. **22**, 833 (1967).

[28]U. Nielsen, R. Haensel, and W. H. E. Schwarz, J. Chem. Phys. **61**, 3581 (1974).

[29]Y. Onodera, J. Phys. Soc. Jpn. **39**, 1482 (1975).

[30]M. W. D. Mansfield, Proc. R. Soc. London, Ser. A **348**, 143 (1976).

[31]P. H. Citrin, G. K. Wertheim, and M. Schlüter, Phys. Rev. B **20**, 3067 (1979).

[32]J. Zaanen, G. A. Sawatzky, J. Fink, W. Speier, and J. C. Fuggle, Phys. Rev. B **32**, 4905 (1985).

[33]W. G. Waddington, P. Rez, I. P. Grant, and C. J. Humphreys, Phys. Rev. B **34**, 1467 (1986).

[34]J. Barth, F. Gerken, and C. Kunz, Phys. Rev. B **28**, 3608 (1983).

[35]J. W. Allen, S. J. Oh, I. Lindau, and L. I. Johansson, Phys. Rev. B **29**, 5927 (1984); S. Cramm, U. Grabowski, C. Kunz, J. Schmidt-May, F. Senf, and L. Incoccia, J. Electron Spectrosc. Relat. Phenomen. **42**, 89 (1987).

[36]B. T. Thole and G. van der Laan, Europhys. Lett. **4**, 1083 (1987).

[37]B. T. Thole and G. van der Laan, Phys. Rev. A (to be published).

[38]D. M. Brink and G. R. Satchler, *Angular Momentum* (Oxford University Press, New York, 1962).

[39]A. de Shalit and I. Talmi, *Nuclear Shell Theory* (Academic, New York, 1963).

[40]I. Lindgren and J. Morrison, *Atomic Many-body Theory*, Vol. 13 of *Springer Series in Chemical Physics* (Springer, New York, 1982).

[41]R. D. Cowan, *The Theory of Atomic Structure and Spectra* (University of California Press, Berkeley, 1981).

[42]R. D. Cowan, J. Opt. Soc. Am. **58**, 808 (1968).

[43]For an introduction to crystal-field theory see, e.g., J. S. Griffith, *The Theory of Transition Metal Atoms* (Cambridge University Press, Cambridge, England, 1971) or A.B.P. Lever, *Inorganic Electronic Spectroscopy* (Elsevier, New York, 1984).

[44]P. H. Butler, *Point Group Symmetry, Applications, Methods and Tables* (Plenum, New York, 1981).

[45]D. W. Lynch and R. D. Cowan, Phys. Rev. B **36**, 9228 (1987).

[46]S. Nakai, K. Ogata, M. Ohashi, C. Sugiura, T. Mitsuishi, and H. Maezawa, J. Phys. Soc. Jpn. **54**, 4034 (1985).

[47]G. van der Laan, J. Zaanen, G. A. Sawatzky, R. C. Karnatak, and J. M. Esteva, Phys. Rev. B **33**, 4253 (1986).

[48]J. R. Derome and W. T. Sharp, J. Math. Phys. **6**, 1584 (1965); P. H. Butler and B. G. Wybourne, Int. J. Quantum Chem. **10**, 581 (1976).

[49]E. V. Sampathkumaran, K. H. Frank, G. Kalkowski, G. Kaindl, M. Domke, and G. Wortmann, Phys. Rev. B **29**, 5702 (1984); W. D. Brewer, G. Kalkowski, G. Kaindl, and F. Holtzberg, Phys. Rev. B **32**, 3676 (1985).

[50]G. van der Laan, J. C. Fuggle, M. P. van Dijk, A. J. Burggraaf, J. M. Esteva, and R. C. Karnatak, J. Phys. Chem. Solids **47**, 413 (1986).

[51]G. Kaindl, G. Kalkowski, E. V. Sampathkumaran, F. Holtzberg, and A. Schach v. Wittenau, J. Magn. Magn. Mater. **47&48**, 181 (1985).

[52]J. Kanski and G. Wendin, Phys. Rev. B **24**, 4977 (1981).

[53]J. M. Esteva, R. C. Karnatak, J. C. Fuggle, and G. A. Sawatzky, Phys. Rev. Lett. **50**, 910 (1983).

[54]B. L. Henke, P. Lee, T. J. Tanaka, R. L. Shimabukuro, and B. K. Fujikawa, At. Data Nucl. Data Tables **27**, 1 (1982).

[55]E. J. McGuire, Phys. Rev. A **5**, 1043 (1972).

[56]J. C. Fuggle and S. F. Alvarado, Phys. Rev. A **22**, 1615 (1980).

[57]G. van der Laan, in *Giant Resonances in Atoms, Molecules and Solids*, edited by J. P. Connerade (Plenum, New York, 1987), p. 447.

[58]M. Benfatto, A. Bianconi, I. Davoli, I. Incoccia, S. Mobilio, and S. Stizza, Solid State Commun. **46**, 367 (1983).

[59]See, e.g., *X-Ray Absorption: Principles, Applications and Techniques of EXAFS, SEXAFS and XANES*, edited by R. Prins and R. Koningsberger (Wiley, New York, 1988).

[60]J. Sugar, W. D. Brewer, G. Kalkowski, G. Kaindl, and E. Paparazzo, Phys. Rev. A **32** 2242 (1985).

[61]G. van der Laan, B. T. Thole, G. A. Sawatzky, J. C. Fuggle, R. C. Karnatak, J. M. Esteva, and B. Lengeler, J. Phys. C **19**, 817 (1986).

[62]M. Piacentini, V. Grasso, S. Santangelo, M. Fanfoni, S. Modesti, and A. Savoia, Solid State Commun. **51**, 467 (1984).

[63]C. Mariani, U. del Pennino, and S. Valeri, Solid State Commun. **61**, 1 (1987).

[64]R. Brydson, B. G. Williams, W. Engel, H. Sauer, E. Zeitler, and J. M. Thomas, Solid State Commun. **64**, 609 (1987).
[65]J. C. Fuggle (unpublished results).
[66]G. van der Laan, M. P. Bruijn, J. B. Goedkoop, and A. A. MacDowell, Proc. Soc. Photo-Opt. Instrum. Eng. **733**, 354 (1987).
[67]G. van der Laan, J. B. Goedkoop, and A. A. MacDowell, J. Phys. E **20**, 1496 (1987).
[68]G. van der Laan, B. T. Thole, G. A. Sawatzky, and M. Verdaguer, Phys. Rev. B **37**, 6587 (1988).
[69]E. E. Koch, Y. Jugnet, and F. J. Himpsel, Chem. Phys. Lett. **116**, 7 (1985).
[70]B. T. Thole, G. van der Laan, and G. A. Sawatzky, Phys. Rev. Lett. **55**, 2086 (1985).
[71]G. van der Laan, B. T. Thole, G. A. Sawatzky, J. B. Goedkoop, J. C. Fuggle, J. M. Esteva, R. C. Karnatak, J. P. Remeika, and H. A. Dabkowska, Phys. Rev. B **34**, 6529 (1986).
[72]G. Schütz, W. Wagner, W. Wilhelm, P. Kienle, R. Zeller, R. Frahm, and G. Materlik, Phys. Rev. Lett. **58**, 737 (1987).
[73]J. B. Goedkoop, B. T. Thole, G. van der Laan, G. A. Sawatzky, F. M. F. de Groot, and J. C. Fuggle, Phys. Rev. B **37**, 2086 (1988).
[74]M. J. Bedzyk and G. Materlik, Phys. Rev. B **32**, 4228 (1985).